Tumor Rejection Induced by CD70-mediated Quantitative and Qualitative Effects on Effector CD8+ T Cell Formation

Ramon Arens,[1,2] Koen Schepers,[3] Martijn A. Nolte,[1,2] Michiel F. van Oosterwijk,[1,2] René A.W. van Lier,[1] Ton N.M. Schumacher,[3] and Marinus H.J. van Oers[2]

[1]Laboratory for Experimental Immunology and [2]Department of Hematology, Academic Medical Center, University of Amsterdam, 1100 DD Amsterdam, Netherlands
[3]Division of Immunology, Netherlands Cancer Institute, 1066 CX Amsterdam, Netherlands

Abstract

In vivo priming of antigen-specific CD8+ T cells results in their expansion and differentiation into effector T cells followed by contraction into a memory T cell population that can be maintained for life. Recent evidence suggests that after initial antigenic stimulation, the magnitude and kinetics of the CD8+ T cell response are programmed. However, it is unclear to what extent CD8+ T cell instruction in vivo is modulated by costimulatory signals. Here, we demonstrate that constitutive ligation of the tumor necrosis factor receptor family member CD27 by its ligand CD70 quantitatively augments CD8+ T cell responses to influenza virus infection and EL-4 tumor challenge in vivo by incrementing initial expansion and maintaining higher numbers of antigen-specific T cells in the memory phase. Concomitantly, the quality of antigen-specific T cells improved as evidenced by increased interferon (IFN)-γ production and a greater cytotoxic potential on a per cell basis. As an apparent consequence, the superior effector T cell formation induced by CD70 protected against a lethal dose of poorly immunogenic EL4 tumor cells in a CD8+ T cell– and IFN-γ–dependent manner. Thus, CD70 costimulation enhances both the expansion and per cell activity of antigen-specific CD8+ T cells.

Key words: costimulation • influenza virus • tumor immunity • MHC tetramer • TNF family member

Introduction

In response to viruses, intracellular bacteria, and a wide range of tumors, antigen-specific CD8+ T cells have to expand for host defense (1, 2). Characteristically, an antigen-specific CD8+ T cell response consists of three phases. In the expansion phase, antigen-specific T cells rapidly increase in numbers by cell divisions, and effector functions are acquired. After viral clearance, ∼90% of the effector T cells are eliminated by apoptosis. This contraction phase gradually converts into the maintenance phase, in which the surviving antigen-specific T cells form the long-lived memory CD8+ T cell population (3, 4).

After initiation, the transition through these stages of CD8+ T cell development is directed by an instructional program that commits CD8+ T cells to proceed with their differentiation (5–8). The duration of antigenic stimulation appears to determine whether clonal expansion is abortive or extensive (9). The fine-tuning mechanisms on the phases and quality of this program have been poorly investigated. Thus far, it has been shown that the cytokine IL-2 delays the contraction phase (10), whereas the opposite has been found for IFN-γ (11). Although it can be assumed that signals transmitted via costimulatory receptors also influence this instructional program, for many costimulatory interactions, the nature of these changes has not been established.

The TNF receptor family member CD27 is constitutively expressed on the majority of T cells and on subsets of antigen-experienced B cells, NK cells, and hematopoietic progenitor cells (12–15). In contrast, expression of its ligand CD70 is tightly regulated and only transiently found on activated lymphocytes and dendritic cells (16–18). In vitro studies showed that CD27–CD70 interactions are in-

volved in T cell expansion (12, 19, 20) and in the enhancement of differentiation of $CD8^+$ T cells into effector cytotoxic T cells (21–23). Studies with $CD27^{-/-}$ mice revealed impaired expansion of antigen-specific T cells in primary and memory T cell responses to influenza virus infection (24). Complementary to these results, increased generation of effector-type T cells was found in B cell–specific CD70 transgenic (Tg) mice that was dependent on TCR triggering (25, 26). Here, we addressed the question whether CD27–CD70 interactions modify quantitative and qualitative aspects of the instructional program of antigen-specific $CD8^+$ T cell development. The results show that CD27 triggering enhances both the expansion and the functional activity of antigen-specific effector T cells. As an apparent consequence of this, CD70 Tg mice are protected from otherwise lethal tumors.

Materials and Methods

Mice

C57BL/6 (wild-type), $CD27^{-/-}$ CD70 Tg (25), F5 TCR Tg (27), $IFN-\gamma^{-/-}$ (28), Ly5.1 mice, and CD70 Tg mice crossed with F5 TCR Tg or $IFN-\gamma^{-/-}$ mice were maintained at the animal department of the Netherlands Cancer Institute. All mice were on a C57BL/6 background. All mice used were 6–9 wk of age and handled in accordance with institutional and national guidelines.

Antibodies, Tetramers, and Peptides

The following monoclonal antibodies were used: allophycocyanin-conjugated anti-CD8 (clone 53-6.7; BD Biosciences), FITC-conjugated anti-CD43 (clone 1B11; BD Biosciences), allophycocyanin-conjugated anti–IFN-γ (clone XMG1.2; BD Biosciences), PE-conjugated Vβ11 TCR (clone RR3-15; BD Biosciences), PE-conjugated mouse anti–human granzyme B (clone GB11; CLB), and PE-conjugated mouse IgG1 isotype control (Becton Dickinson). Rat anti–mouse CD4 (clone GK1.5) and rat anti–mouse CD8 (clone 2.43) used in depletion experiments as well as rat anti–mouse CD8 (clone 53-6.7) used for immunohistochemistry and hamster anti–mouse CD27 (clone LG.3A10) were purified from hybridoma culture supernatant. $F(ab)_2$ fragments of the CD27 mAb were prepared and FITC labeled according to standard procedures. The influenza virus-specific $H2-D^b-NP_{366-374}$ and $H2-D^b-PA_{224-233}$, and the Moloney virus–specific $H2-D^b-GagL_{85-93}$ tetramers were prepared as described previously (29–31). The nucleoprotein (NP)-derived peptide ASNENMDAM (366–374) was produced using standard F-moc chemistry.

Virus Infection and Adoptive Transfers

Purified influenza A virus was provided by R. Consalves (National Institute for Medical Research, London, England, UK) and grown in the Department of Virology at Erasmus University. Mice were anesthetized and infected intranasally with 25 HAU of influenza virus. Detection of influenza virus in lung homogenates was done using real-time quantitative PCR as described previously (32).

For adoptive transfers, $CD8^+$ T cells were purified from spleens of F5 TCR Tg mice and F5 TCR Tg $\times$ CD70 Tg mice by negative selection using the MACS separation system as described previously (25). Cells were either unlabeled or labeled with 2 μm carboxyfluorescein succinimidyl ester (CFSE) in PBS at 37°C for 10 min and injected i.v. into Ly5.1 recipient mice.

Where indicated, recipient mice were infected with influenza virus 1 d after adoptive transfer.

Tumor Challenge and T Cell Depletion

Tumor cells used were EL4, EL4-NP, and EL4–green fluorescent protein (GFP; reference 33). Tumor cells were maintained in IMDM supplemented with 5% heat-inactivated FCS, 5×10^{-5} M β-mercaptoethanol, 100 U/ml penicillin, and 100 μg/ml streptomycin. Mice were challenged s.c. in the right flank with 10^6 tumor cells. Every 3–4 d, tumor size was measured in two dimensions. Mice were killed when tumors reached diameters >15 mm.

In vivo depletion of $CD4^+$ and $CD8^+$ T cells was accomplished by intraperitoneal injections with 0.6 mg of rat anti–mouse CD4 mAb (clone GK1.5) or 0.6 mg rat anti–mouse CD8 mAb (clone 2.43), respectively, at days −4, 0, 3, 7, 9, 12, and 15 in relation to tumor challenge. The absence of $CD4^+$ or $CD8^+$ T cells was determined by FACS® analysis with FITC-conjugated anti-CD4 (clone MT4) and PE-conjugated anti-CD8 (clone 53–6.7), respectively.

Detection of Antigen-specific Immune Responses and Cytotoxicity Assay

Flow Cytometry. At indicated time points, blood was drawn from the tail vein, and single cell suspensions from spleen, LNs, lungs, and tumors were obtained by mincing through cell strainers. Erythrocytes in spleen and blood were lysed with ammonium chloride solution. Cells were counted and incubated at room temperature for 15 min with antibodies and tetramers. Live cells were selected based on 2 μg/ml propidium iodide exclusion. Absolute numbers of antigen-specific T cells were calculated from the frequency of $H-2D^b$ tetramer$^+$ $CD8^+$ cells and the total numbers of cells recovered. Intracellular staining for granzyme B was performed with PE-labeled mouse anti–human granzyme B and PE-labeled mouse IgG1 (isotype control) using a Cytofix/Cytoperm Kit (BD Biosciences) according to the manufacturer's guidelines. Flow cytometric analyses were performed on a FACSCalibur™ using CELLQuest™ software (Becton Dickinson). Statistical analyses were performed with a two-tailed Student's t test.

Intracellular Cytokine Staining. 10^6 cells/well spleen cells were stimulated for 5 h at 37°C and in 5% CO_2 conditions in flat-bottom 96-well plates in 200 μl IMDM (Life Technologies) with 20 U/ml of recombinant human IL-2 and 1 μg/ml brefeldin A (Sigma-Aldrich) in the presence or absence of 1 μg/ml $NP_{366-374}$ peptide. After stimulation, cells were first surface stained for CD8, and subsequently intracellular cytokine staining was performed for IFN-γ using a Cytofix/Cytoperm Kit (BD Biosciences) according to the manufacturer's guidelines.

Flow Cytometry CTL Assay. The flow cytometry CTL assay (OncoImmunin; reference 34) was performed according to the guidelines from the manufacturer with some modifications as described in this paragraph. To obtain effector cells, spleens of wild-type and CD70 Tg mice challenged with EL4-NP tumor cells were collected at day 9 after tumor challenge, and single cell suspensions were prepared by mincing through cell strainers. T cells were purified using Thy1.2 microbeads and the MACS system (Miltenyi Biotec). Purified T cells (>95%) were stained with CD8 mAb and $H-2D^b-NP_{366-374}$ tetramers to define effector cell numbers (i.e., $NP_{366-374}$-specific $CD8^+$ cells). Target cells (EL4 cells) were suspended in IMDM containing 10% FCS at 10^6 cells/ml, fluorescently labeled, and pulsed with 10 μg/ml $NP_{366-374}$ peptide for 1 h at 37°C and in 5% CO_2 conditions. Target cells were incubated with effector cells at various effector/target cell ratios in a 96-well plate for 2.5 h at 37°C in a 5% CO_2 incubator.

After washing, cells were incubated with caspase substrate for 40 min, washed, and analyzed by flow cytometry.

Immunohistochemistry

CD8^{+} T cell infiltrates in tumor tissue were assessed by immunohistochemistry. Tumors were cut into pieces and frozen in TissueTek (Sakura Finetek) at −70°C, and 6-μm cryostat sections were prepared. These sections were applied on gelatin-coated microscope glass slides, fixed in dehydrated acetone for 10 min, air dried, and rehydrated with 2% newborn calf serum in PBS. The sections were incubated for 45 min with biotinylated rat anti–mouse CD8 mAb, washed three times with PBS, and subsequently incubated for 30 min with Alexa 594–conjugated streptavidin (Molecular Probes). Sections were washed with PBS, and

nuclei were counterstained with Hoechst 33342 and finally coverslipped with Fluorostab (ICN/Cappel). Fluorescence was analyzed using a microscope (Eclipse model E800; Nikon) connected to a digital camera.

Online Supplemental Material

Fig. S1 shows the B and T cell phenotype of the CD70 Tg mice at the time of the antigenic challenge. Splenocytes of 6-wk-old wild-type and CD70 Tg mice were isolated and analyzed by flow cytometry for CD70 and B220 expression (Fig. S1 A), CD27 and Thy1.2 expression (Fig. S1 B), and CD43 (1B11) and NP$_{366-374}$ tetramer expression (Fig. S1 C, gated on CD8^{+} T cells). Online supplemental material is available at http://www.jem.org/cgi/content/full/jem.20031111/DC1.
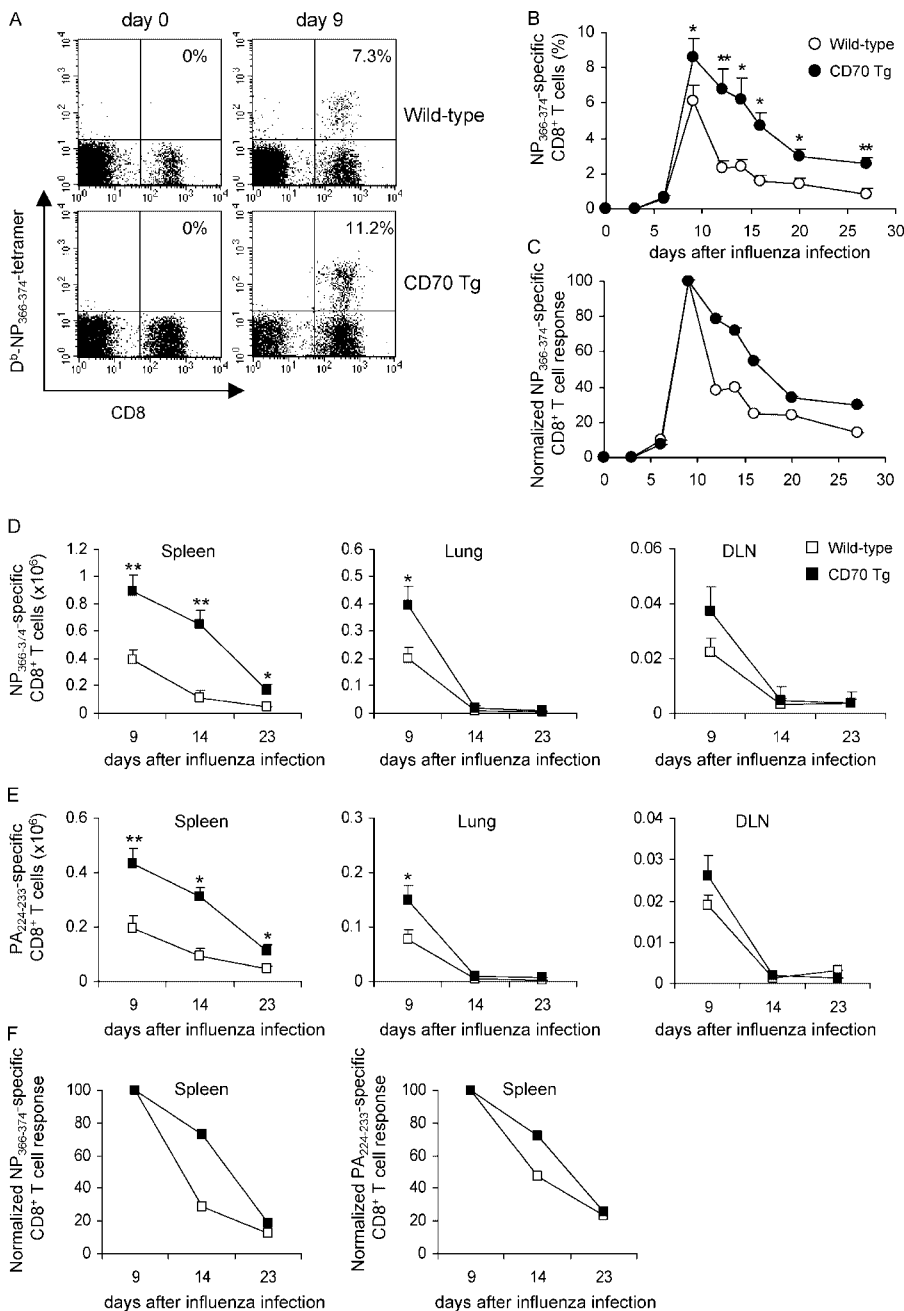
Figure 1. Increased generation of antigen-specific CD8^{+} T cells in CD70 Tg mice after influenza virus infection. Wild-type and CD70 Tg mice were infected intranasally with influenza virus. (A) Representative FACS® profiles of blood cells collected at day 0 and at day 9 after infection showing H-2D^b-NP$_{366-374}$ tetramer staining versus CD8. Numbers indicate the percentages of H-2D^b-NP$_{366-374}$–specific cells within the CD8^{+} T cell compartment. No cells were stained with Moloney virus–specific (H-2D^b-GagL$_{85-93}$) tetramers (not depicted). (B) Frequency of H2-D^b-NP$_{366-374}$ tetramer positive cells among CD8^{+} T cells in blood at the indicated days after influenza virus infection. Data represent mean values and standard error from 10 mice per group. Significance of differences was determined by two-tailed Student's t test (*, P < 0.05; **, P < 0.005). (C) Expansion and contraction of NP$_{366-374}$–specific CD8^{+} T cells in blood was normalized to the peak of the response (at day 9). (D) Absolute numbers of NP$_{366-374}$-specific and (E) PA$_{224-233}$-specific CD8^{+} T cells in spleens, DLNs, and lungs 9 d after infection. Data representing the mean and standard error from six mice per group are shown. Significance of differences was determined by two-tailed Student's t test (*, P < 0.05; **, P < 0.005). Both groups of mice showed no difference in kinetics of viral clearance. (F) Contraction of antigen-specific CD8^{+} T cells in the spleen was normalized to the peak of the response (at day 9).

Results

Increased Antigen-specific Effector CD8$^+$ T Cell Expansion in CD70 Tg Mice after Influenza Infection. To test the impact of CD27 ligation on the kinetics of the immune reaction in a physiological virus infection model, influenza virus–specific CD8$^+$ T cell responses of intranasally influenza virus–infected wild-type and CD70 Tg mice were compared longitudinally using MHC class I tetramers. At the peak of the response, at day 9 after infection, influenza-specific CD8$^+$ T cell frequencies as measured by NP$_{366-374}$ tetramer staining in peripheral blood were moderately increased in CD70 Tg mice as compared with wild-type mice (Fig. 1, A and B). Analyses of the ensuing time points revealed a modest delay in contraction of the influenza-specific CD8$^+$ T cell pool in peripheral blood of CD70 Tg mice (Fig. 1, B and C). Finally, percentages of tetramer-binding T cells remaining long after viral clearance (day 27) were significantly higher in the CD70 Tg mice than in wild-type mice (Fig. 1 B). The kinetics and magnitude of the influenza-specific CD8$^+$ T cells paralleled the expression of the effector cell marker 1B11 (35), recognizing the activation-associated glycoform of CD43 on the total CD8$^+$ T cell population (unpublished data).

At the peak of the response, the absolute numbers of NP$_{366-374}$-specific CD8$^+$ T cells in spleen and lung were significantly increased in CD70 Tg mice as compared with wild-type mice (Fig. 1 D). In lung/draining LNs (DLNs), the absolute numbers of NP$_{366-373}$-specific CD8$^+$ T cells were slightly but not significantly increased in CD70 Tg mice (Fig. 1 D). Comparable results were obtained with tetramers loaded with the PA$_{224-233}$ epitope of influenza virus (Fig. 1 E). Although no difference in contraction of the influenza virus–specific CD8$^+$ T cell populations in lung and DLNs was found, a modest delay in contraction of NP$_{366-373}$- and PA$_{224-233}$-specific CD8$^+$ T cell populations in the spleen was observed (Fig. 1 F). To exclude the possibility that the increased numbers of antigen-specific CD8$^+$

T cells in the CD70 Tg mice were caused by differences in viral clearance, we determined the viral titers in the lung of infected mice at several time points. At day 9 after infection, the viral titers were not significantly different. If anything, viral titers were lower in CD70 Tg mice compared with wild-type mice (unpublished data). At days 14 and 23 after viral infection in both groups of mice, no virus could be detected anymore.

The aforementioned results indicate that constitutive CD70 expression enhances the expansion of antigen-specific CD8$^+$ T cells upon influenza virus infection. These findings might either be due to a broadening of the T cell repertoire specific for a given influenza antigen or to increased accumulation of the progeny of a similar repertoire of T cells. To determine the effects of constitutive CD70 expression on a monoclonal antigen-specific CD8$^+$ T cell population, we bred mice Tg for the MHC class I–restricted TCR recognizing the influenza virus epitope NP$_{366-374}$ (F5 TCR Tg; reference 27) with CD70 Tg mice. After influenza infection, F5 TCR Tg $\times$ CD70 Tg mice showed increased frequencies of CD8$^+$ T cells with a CD43^{hi} effector phenotype in peripheral blood as compared with F5 TCR Tg mice. This started at day 2 after infection and was maintained until day 31 (Fig. 2 A). At the peak of the response, at approximately day 9 after infection, frequencies as well as absolute numbers of CD43^{hi}CD8$^+$ effector T cells were significantly increased in both spleen and DLNs, but not in lung tissue of F5 TCR Tg $\times$ CD70 Tg as compared with F5 TCR Tg mice (Fig. 2, B and C), indicating that CD70 costimulation also enhances expansion of monoclonal CD8$^+$ T cells. This excludes the possibility that our data can be explained by a CD70-mediated, TCR triggering–independent polyclonal T cell activation.

To establish whether the CD70-mediated increase in antigen-specific CD8$^+$ T cell responses is dependent on its interaction with CD27, we challenged CD70 Tg mice on a
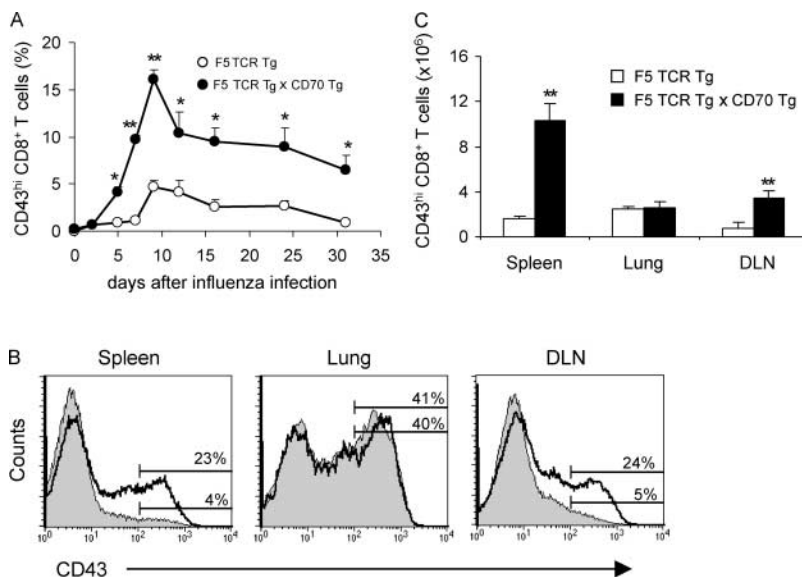
Figure 2. Increased effector CD8$^+$ T cells in NP-specific TCR Tg $\times$ CD70 Tg mice. F5 TCR Tg and F5 TCR Tg $\times$ CD70 Tg mice were infected intranasally with influenza virus. (A) Frequency of CD43^{hi}-expressing CD8$^+$ T cells in blood at the indicated days after influenza virus infection. Data represent mean values and standard error of five mice per group. Significance of differences was determined by two-tailed Student's *t* test (*, P < 0.05; **, P < 0.005). (B) Representative FACS® profiles of spleen, lung, and DLNs collected at day 9 after influenza virus infection showing CD43 staining on gated CD8$^+$ T cells of TCR Tg mice (shaded histograms) and TCR Tg $\times$ CD70 Tg mice (solid lines). Numbers indicate the percentage of CD43^{hi} cells within the CD8$^+$ T cell compartment. (C) Absolute numbers of CD43^{hi}CD8$^+$ T cells in spleen, lung, and DLNs at day 9 after infection. Data represent mean values and standard error of five mice per group. Significance of differences was determined by two-tailed Student's *t* test (**, P < 0.005).
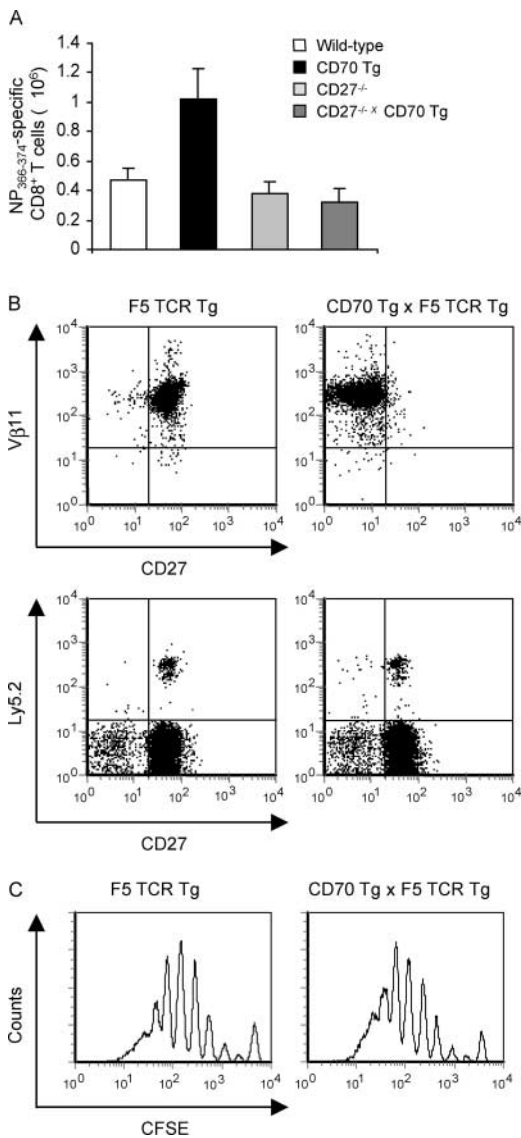
Figure 3. CD70-mediated effects on antigen-specific CD8$^+$ T cell responses require CD27 stimulation during antigen encounter. (A) Wild-type, CD27$^{-/-}$, CD70 Tg, and CD27$^{-/-}$ × CD70 Tg mice were infected intranasally with influenza virus. At day 9 after infection, spleens were collected, and absolute numbers of NP$_{366-374}$-specific CD8$^+$ T cells were determined. (B) Reduced CD27 expression on T cells in CD70 Tg × TCR Tg mice requires continuous triggering by CD70. Splenic CD8$^+$ T cells from F5 TCR Tg mice and F5 TCR Tg × CD70 Tg mice were purified and stained with mAbs specific for Vβ11 and CD27 (top). 1 d after adoptive transfer of 4 × 10^6 purified CD8$^+$ T cells from F5 TCR Tg mice and F5 TCR Tg × CD70 Tg mice into Ly5.1 mice, spleen cells were stained with mAbs specific for CD8, CD27, and Ly5.2 (bottom). Dot plots are gated on CD8$^+$ T cells. (C) Purified CD8$^+$ T cells from F5 TCR Tg mice and F5 TCR Tg × CD70 Tg mice were CFSE-labeled and adoptively transferred into Ly5.1 recipient mice. At 1 d after transfer, mice were infected with influenza virus. 4 d after virus infection, DLN cells were stained with mAbs specific for CD8 and Ly5.2. Flow cytometric histograms of CFSE dilution on CD8 and Ly5.2-positive cells are shown.

CD27-deficient background with influenza virus. The observed increase in the numbers of splenic influenza-specific CD8$^+$ T cells in CD70 Tg mice was not found in

CD27$^{-/-}$ × CD70 Tg mice (Fig. 3 A), indicating an absolute requirement for CD27.

The expression of CD27 is low to undetectable in CD70 Tg and F5 TCR Tg × CD70 Tg mice at the time of TCR triggering (Fig. 3 B and Fig. S1, available at http://www.jem.org/cgi/content/full/jem.20031111/DC1). Therefore, the effects observed in the CD70 Tg mice could either be explained by constitutive triggering of CD27 via CD70 or by CD70-induced presensitization of the T cells, resulting in an increased responsiveness at the time of antigen encounter. To determine whether CD27 is permanently lost on T cells in CD70 Tg mice, or whether the absence of CD27 cell surface expression is due to continuous triggering by CD70, we analyzed CD27 expression on T cells of F5 TCR Tg and F5 TCR Tg × CD70 Tg mice after adoptive transfer into wild-type mice. Within 24 h after adoptive transfer, CD27 expression was found on both adoptively transferred T cell populations (Fig. 3 B). CD27 expression was also detectable on both TCR Tg and TCR Tg × CD70 Tg T cells after 1 d of in vitro culture in the presence of concanavalin A (unpublished data). These data indicate that the T cells in CD70 Tg mice continue to produce CD27, but downmodulate the molecule due to continuous interaction with CD70.

To determine whether CD27 ligation by CD70 could have presensitized T cells, CD8$^+$ T cells of F5 TCR Tg and F5 TCR Tg × CD70 Tg mice were labeled with CFSE, a fluorescent dye that is diluted with each cell division, and injected into Ly5.1 recipient mice that were infected with influenza virus 1 d later. No significant differences were observed in CFSE dilution between DLN T cells from F5 TCR Tg mice and from TCR Tg × CD70 Tg mice at day 4 after infection (Fig. 3 D, 55 ± 21% F5 TCR Tg T cells with ≥6 cell cycle divisions vs. 67 ± 18% F5 TCR Tg × CD70 Tg T cells; $n = 8$). In addition, no significant differences in absolute numbers of influenza-specific CD8$^+$ T cells between the two groups were observed at days 5 and 7 after influenza infection (unpublished data). Collectively, these data indicate that the CD70-mediated effects on antigen-specific T cell responses can be explained by constitutive CD27 ligation during antigenic challenge rather than a presensitizing effect of CD27–CD70 interactions. Overall, triggering of CD27 augments initial expansion, modestly delays the contraction phase, and maintains higher numbers of CD8$^+$ T cells in the memory stage upon influenza virus infection.

Increased Antigen-specific CD8$^+$ T Cell Expansion upon Tumor Challenge. The effects of CD27 ligation in vivo on antitumor CD8$^+$ T cell responses were analyzed using EL4 tumor cells that express the influenza A virus–derived NP$_{366-374}$ epitope. These tumor cells induce an NP$_{366-374}$-specific CD8$^+$ T cell response and tumor rejection in normal mice (33). Subcutaneously inoculated EL4–NP tumor cells were rejected in wild-type and CD70 Tg mice with similar kinetics (Fig. 4 A). The percentage of NP$_{366-374}$-specific CD8$^+$ T cells at the peak of the response (day 13 after tumor challenge) and on consecutive days, was increased
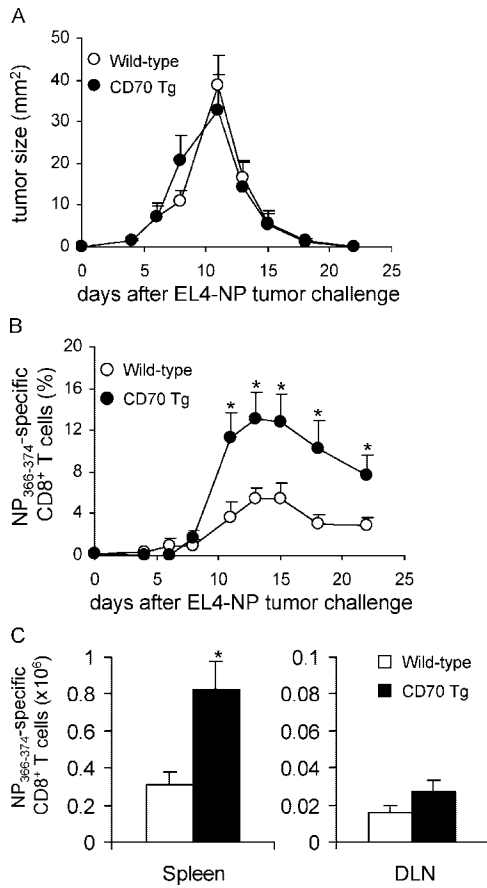
Figure 4. Increased generation of NP-specific CD8$^+$ T cells in CD70 Tg mice after EL4-NP tumor challenge. (A) Wild-type and CD70 Tg mice were challenged subcutaneously with 10^6 EL4-NP tumor cells, and tumor size was measured at the indicated days after tumor challenge. Data represent mean values and standard error of six mice per group. (B) Frequency of NP$_{366-374}$-specific CD8$^+$ T cells in blood of wild-type and CD70 Tg mice. Significance of differences was determined by two-tailed Student's t test (*, P < 0.05). (C) Absolute numbers of NP$_{366-374}$-specific CD8$^+$ cells in spleen and DLNs at day 13 after tumor challenge. Significance of differences was determined by two-tailed Student's t test (*, P < 0.05).

approximately two- to threefold in the blood of CD70 Tg mice (Fig. 4 B). Similarly, the absolute number of NP$_{366-374}$-specific CD8$^+$ T cells was significantly increased in the spleen of CD70 Tg mice and slightly increased in DLNs (Fig. 4 C). As in influenza infection, increased percentages of CD43^{hi}CD8$^+$ T cells were observed in the peripheral lymphoid organs of CD70 Tg mice (unpublished data). It is unlikely that the B cell depletion occurring in CD70 Tg mice (25) is involved in the observed effects on CD8$^+$ T cell responses because B cell–deficient mice show similar CD8$^+$ T cell responses after EL4-NP challenge (unpublished data). Together, these data show that CD27 stimulation augments the expansion and maintenance of the antigen-specific T cell pool after tumor challenge.

Increased Acquisition of Effector Cell Properties after CD27 Ligation. It is unconfirmed whether signals transmitted via TNF receptor family members improve effector T cell responses in a qualitative fashion (36). To assess whether

CD27 stimulation contributes to the competence of antigen-specific T cells, we analyzed the acquisition of effector cell properties of NP$_{366-374}$-specific T cells directly ex vivo. At the peak of the CD8$^+$ T cell response to EL4-NP tumor cells, splenic NP$_{366-374}$-specific CD8$^+$ T cells were analyzed for their capacity to produce IFN-γ and TNF-α after in vitro stimulation with NP$_{366-374}$ peptide. The percentage of splenic CD8$^+$ T cells producing IFN-γ after NP$_{366-374}$ peptide stimulation was significantly increased in CD70 Tg mice (4.1 ± 1.0% in wild-type vs. 7.2 ± 1.2% in CD70 Tg mice; $n = 5$, P < 0.05). This may in large part be explained by the increased size of the antigen-specific CD8$^+$ T cell compartment. Remarkably, the IFN-γ production on a per cell basis was reproducibly higher (Fig. 5 A, 316 ± 68 mean fluorescence intensity (MFI) wild-type vs. 582 ± 98 MFI CD70 Tg mice; $n = 5$, P < 0.05). Constitutive CD27 ligation had no effect on TNF-α production in CD8$^+$ T cells (Fig. 5 A). The contribution of CD27–CD70 interaction to the development of cytotoxic activity to NP$_{366-374}$ peptide–loaded EL4 cells was examined using a recently described flow cytometric CTL assay (34). On a per cell basis, the ex vivo cytotoxicity of splenic NP-specific CD8$^+$ T cells was enhanced in CD70 Tg mice as compared with wild-type mice (Fig. 5, B and C). Furthermore, the increase in cytotoxic activity in T cells of CD70 Tg mice was associated with augmented granzyme B expression in both CD8$^+$ T cells and NP-specific CD8$^+$ T cells in terms of intensity and percentages (Fig. 5 D). As predicted, granzyme B expression was primarily found in the CD43$^+$ effector T cell subset. Also, after influenza infection, splenic antigen-specific CD8$^+$ T cells in CD70 Tg mice had increased IFN-γ expression and cytotoxic activity (unpublished data). Thus, apart from increasing the size of the effector T cell pool, CD27 stimulation enhances the capacity of CD8$^+$ effector T cells to produce IFN-γ and to execute cytolysis of antigen-bearing target cells.

CD8$^+$ T Cell– and IFN-γ–dependent Tumor Regression in CD70 Tg Mice. The aforementioned findings showed that in the presence of a strong CD27 signal, both quantity and quality of CD8$^+$ T cell responses improve. To evaluate the possible benefits of this for increased immunity, the ability of CD8$^+$ T cells to control growth of poorly immunogenic tumors was evaluated in CD70 Tg and wild-type mice. In view of this purpose, we examined the response to EL4 tumor cells and EL4 tumor cells transduced with a retroviral vector containing GFP and the Moloney-derived MHC class I–restricted GagL$_{85-93}$ epitope. The GagL epitope encoded by the Moloney retrovirus is derived from an alternative translation initiation site, and presentation of this epitope is insufficient to allow immune control of EL4-GFP tumors in wild-type mice (33). EL4 and EL4-GFP tumor cells grew progressively in wild-type mice, whereas in CD70 Tg mice, both EL4 and EL4-GFP tumors regressed at day 9 after tumor inoculation (Fig. 6, A and B). At day 9 after tumor challenge, spleens and tumors of CD70 Tg mice challenged with EL4-GFP contained increased percentages of tumor-specific CD8$^+$ T cells as compared with wild-type
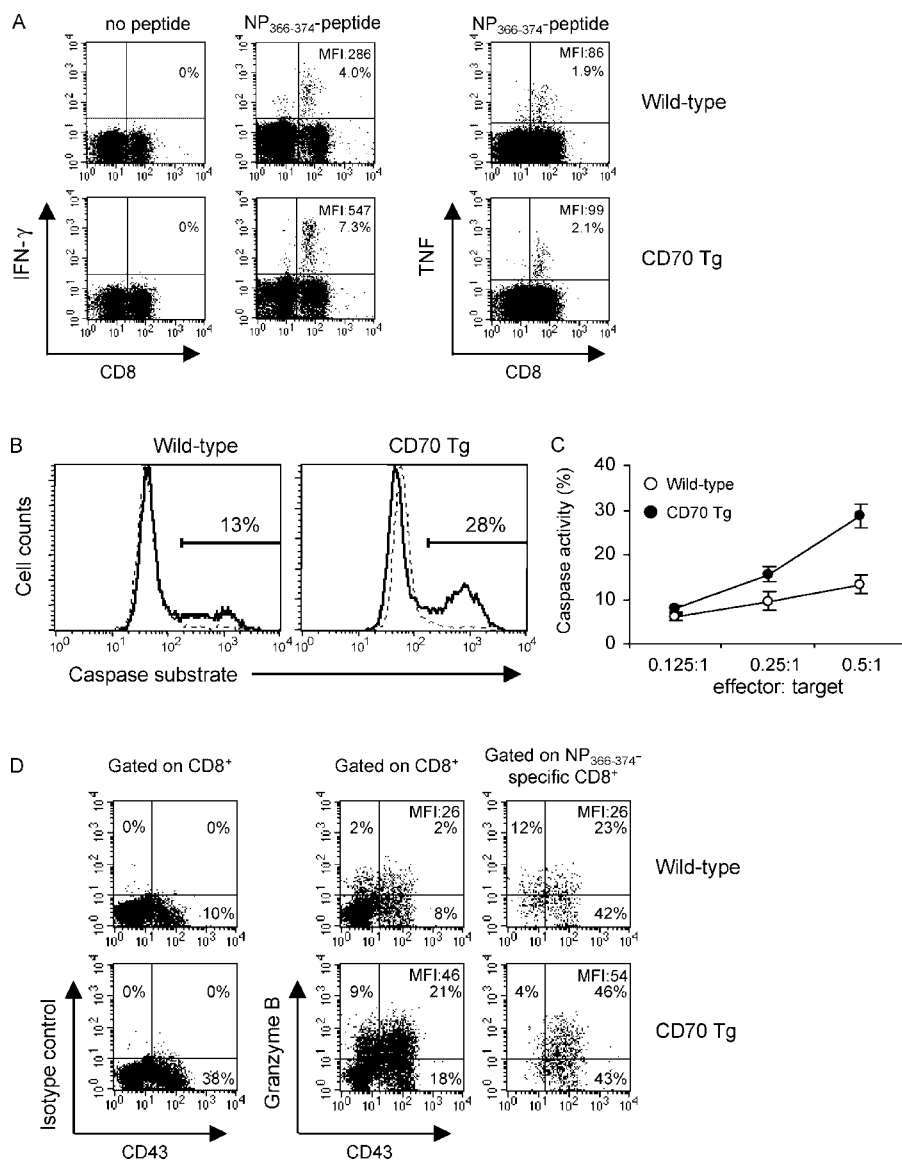
Figure 5. Increased IFN-γ production and cytotoxic activity in CD70 Tg mice. Phenotypic analysis of splenic CD8⁺ T cells of wild-type and CD70 Tg mice collected 12 d after challenge with 10⁶ EL4-NP tumor cells. (A) Intracellular IFN-γ and TNF-α staining of NP₃₆₆₋₃₇₄-specific CD8⁺ T cells. Intracellular IFN-γ and TNF-α levels were measured in spleen cells after 5 h of incubation in the presence or absence of NP₃₆₆₋₃₇₄ peptide. The percentage and MFI of IFN-γ⁺ and TNF⁺ cells within the CD8⁺ gate are indicated. Background (no peptide) was <0.2%. (B) Cytotoxic activity of NP₃₆₆₋₃₇₄-specific CD8⁺ T cells. Target cells (EL4 cells) were fluorescently labeled, pulsed with NP₃₆₆₋₃₇₄ peptide or unpulsed, and subsequently cocultured with effector cells (NP₃₆₆₋₃₇₄-specific CD8⁺ T cells) at different effector to target cell ratios in which effector populations from wild-type and CD70 Tg mice were equalized based on the percentage of NP-specific cells. Killing of target cells was assessed by a flow cytometric CTL assay detecting the induction of caspase activity in target cells. Histograms are gated on EL4 target cells, and the numbers indicate the percentage caspase positive cells. The solid and dotted lines represent peptide-pulsed or unpulsed target cells, respectively. (C) Measurement of cytotoxicity as described in B with different effector to target cell ratios. Data are displayed as mean and standard error (*n* = 5). (D) Ex vivo intracellular granzyme B staining. CD8⁺ T cells and NP₃₆₆₋₃₇₄-specific CD8⁺ T cells were stained for CD43 and intracellular granzyme B. Gated CD8⁺ and NP₃₆₆₋₃₇₄-specific CD8⁺ T cells are shown. The numbers indicate the percentages of cells within the designated quadrant and are representative of five mice.

mice challenged with EL4-GFP (Fig. 6 C). Furthermore, immunohistochemistry of tumor tissue at day 9 after tumor challenge showed that in CD70 Tg mice, the tumors contained larger infiltrates of CD8⁺ T cells (Fig. 6 D).

To analyze the contribution of the CD4⁺ and CD8⁺ T cell subsets in the CD70-mediated EL4 tumor regression, CD70 Tg mice were treated with either anti-CD4 or anti-CD8 mAbs to deplete CD4⁺ or CD8⁺ T cells. As shown in Fig. 6 E, treatment of CD70 Tg mice with mAb to CD8, but not to CD4, prevented the rejection of tumors in CD70 Tg mice, indicating that CD8⁺ T cells play a key role in the CD70-mediated tumor rejection. When EL4 cells were inoculated subcutaneously in IFN-γ⁻/⁻ mice or IFN-γ⁻/⁻ × CD70 Tg mice, the EL4 cells grew progressively in both strains of mice, indicating a critical requirement for IFN-γ in the CD70-mediated tumor rejection (Fig. 6 F). Together, these results show that CD27 ligation protects against lethal tumor challenge in a CD8⁺ T cell–

and IFN-γ–dependent manner, and this protection can be correlated to an enhanced number and efficacy of tumor-specific effector CD8⁺ T cells.

Discussion

In the present work, we have shown that in vivo costimulation of T cells by constitutive triggering of CD27 by its ligand CD70 results in increased numbers as well as more competent antigen-specific CD8⁺ T cells upon challenge with either influenza virus or EL4-NP₃₆₆₋₃₇₄ cells. Moreover, challenge with a lethal dose of poorly immunogenic EL4 lymphoma cells results in a CD8⁺- and IFN-γ–dependent rejection of the tumor in CD70 Tg mice, but not in wild-type mice.

The observed CD70-mediated enhancement of antigen-specific CD8⁺ T cell responses is both quantitative and qualitative. With respect to the quantitative effects, the in-
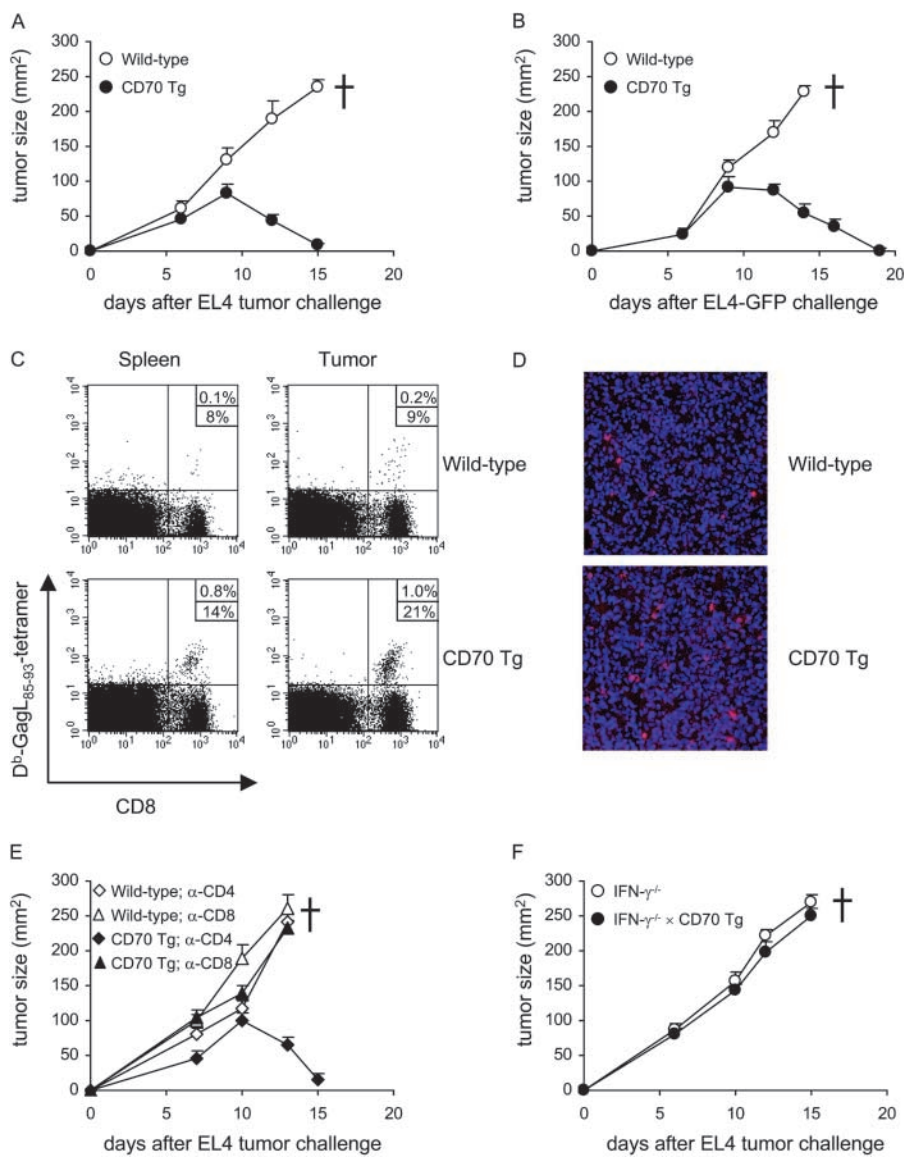
Figure 6. CD8^{+} T cell– and IFN-γ– dependent tumor rejection in CD70 Tg mice. Mice were challenged subcutaneously with 10[6] EL4 or EL4-GFP tumor cells. Tumors were measured, and mice were killed when tumors reached diameters of >15 mm. (A) EL4 and (B) EL4-GFP tumor rejection in CD70 Tg mice. Tumor size of wild-type and CD70 Tg mice was measured at the indicated days after tumor challenge. Data represent mean values and standard error of eight mice per group. (C) Increased frequencies of CD8^{+} T cells and tumor specific-CD8^{+} T cells in spleen and tumors after EL4-GFP challenge as determined using anti-CD8 mAbs and H-2D^b-GagL$_{85-93}$ tetramers at day 9 after tumor challenge. (D) CD8^{+} T cell infiltrates (red) in EL4-GFP tumors (blue) from wild-type and CD70 Tg mice at day 9 after tumor challenge as determined by immunohistochemistry. (E) CD8^{+} T cells are critically involved in EL4 tumor rejection in CD70 Tg mice. Tumor size was measured at the indicated days after EL4 tumor challenge in mice treated with either anti-CD4 or anti-CD8 mAbs. Data represent mean values and standard error from five mice per group. (F) IFN-γ is critically involved in EL4 tumor rejection in CD70 Tg mice. Tumor size of IFN-γ^{-/-} and IFN-γ^{-/-} × CD70 Tg mice was measured at the indicated days after tumor challenge. Data represent mean and standard error from five mice per group.

creased numbers of antigen-specific CD8^{+} T cells in CD70 Tg mice after influenza virus infection and tumor challenge presumably enhance the efficacy of the primary response. Recently, it was shown that the contraction of the CD8^{+} T cell compartment occurs independently of the continuous presence of antigen (8). Here, we have found that constitutive CD27–CD70 interaction results in a modest delay in contraction of influenza-specific CD8^{+} T cells in peripheral blood and spleen (Fig. 1, C and F), indicating that the contraction phase can be modulated by CD8^{+} T cell extrinsic factors (i.e., provided by members of the TNF receptor family). Because endogenous CD70 expression on activated lymphocytes and dendritic cells is transient and under tight control of the presence of antigen, the contribution of CD27 to T cell expansion, maintenance, and contraction will normally depend on the amount and persistence of antigen. Whether the modulation by CD70 takes place at the initiation and/or throughout the different phases of the T cell response remains to be established.

As to the qualitative aspects of in vivo ligation of CD27, we found an increased ex vivo cytotoxic activity of antigen-specific CD8^{+} T cells (Fig. 5, B and C), correlating with a higher granzyme B expression (Fig. 5 D). This finding is consistent with previous in vitro studies (21–23), and shows that CD27–CD70 interactions boost the cytotoxic capacity of CD8^{+} T cells, thereby improving outcome of viral infections and tumor challenge. Finally, the CD27-mediated induction of type 1 IFN-γ–producing T cells (Fig. 5 A) might also contribute to the observed enhanced immunity because these T cells tend to migrate to the site of infection (37). Actually, we have found numerous IFN-γ–producing T cells at the effector site (unpublished data) along with splenic IFN-γ–producing T cells. In addition, IFN-γ secreted by antigen-specific CD8^{+} T cells might further enhance immunity by its pleiotropic effects on the immune system, including increased presentation of peptides by MHC class I (38).

The enhanced CD8^{+} T cell responses by constitutive CD70 expression on B cells is most likely due to direct liga-

tion of CD27 on CD8^{+} T cells rather than CD27 ligation on CD4^{+} T cells, thereby increasing the T helper cell activity for four reasons. First, in viral infections, the primary CD8^{+} T cell responses are known to be unaffected when CD4^{+} T cells are absent (39–41). Second, increased CD8^{+} T cell responses were also observed after influenza infection on a MHC class I–restricted TCR background (Fig. 2). Third, the EL4-NP$_{366-374}$ tumor response is MHC class I restricted and independent of MHC class II (33). Fourth, we have shown here that the rejection of the EL4 tumor in CD70 Tg mice is CD4^{+} T cell independent (Fig. 6 E).

The costimulatory effect of CD27 is dependent on TCR triggering (26), indicating that CD27-derived signals synergize with TCR-derived signals, which may lower the T cell activation threshold for antigenic stimulation. CD27-derived costimulatory signals might also up-regulate antiapoptotic molecules, thereby promoting T cell survival. In fact, we recently found up-regulation of Bcl-x$_L$ expression after CD27 triggering on T cells (unpublished data), which is in line with data obtained with the CD27 relatives OX40 and 4-1BB (42, 43). These data suggest that the prolonged duration of antigen-specific CD8^{+} T cell responses in CD70 Tg mice may at least in part be explained by an antiapoptotic effect of CD27 triggering. In addition, prolonged survival of antigen-specific cells enables these cells to receive additional activation and differentiation signals.

Previously, it was found that absence of CD27–CD70 interaction leads to diminished antigen-specific T cell numbers after influenza virus infection (24). Here, we have found that constitutive CD27 ligation results in increased influenza-specific CD8^{+} T cells during the expansion, contraction, and memory phase by stimulating the progeny of a similar repertoire of T cells. These complementary findings show that CD27–CD70 interactions play a regulatory role in T cell responses to influenza virus. There are no a priori reasons to assume that there is not a similar role for CD27–CD70 interactions in other antiviral responses. In humans with latent CMV infection, the number of antigen-specific CD27^{−} CD8^{+} T cells was found to be linearly related to the total number of CMV-specific CD8^{+} T cells (44). As these CD27^{−} cells are most likely the consequence of interaction with CD70, this suggests a prominent role for CD27–CD70 interaction in driving T cell expansion during viral infections.

Our finding that constitutive CD70 expression on B cells results in improved antitumor immunity is in line with earlier studies showing that tumors transfected with CD70 have an enhanced capacity to induce antitumor immune responses (45–47). Interestingly, our data indicate that CD70 does not need to be present on the tumor itself to have its potent effects on antitumor immunity. Thus, targeting of CD27 might be a therapeutic tool to enhance antigen-specific T cell responses. Because we have shown that chronic stimulation of CD27 eventually results in lethal immunodeficiency due to exhaustion of the naive T cell pool (26), it is essential to regulate the amount and duration of T cell CD27 stimulation in vivo to avoid detrimental effects.

In summary, our work shows that in vivo CD27 ligation

by constitutive CD70 expression on B cells enhances the primary CD8^{+} T cell response to influenza virus and tumors. CD27 stimulation results in increased antigen-specific CD8^{+} T cell numbers and in increased IFN-γ production as well as increased cytotoxicity on a per cell basis. This suggests that CD27 stimulation by CD70, even when presented outside the viral or tumor environment, may prove useful as a strategy for enhancing CD8^{+} T cell responses to viruses and tumors.

References

1. Sprent, J., and C.D. Surh. 2002. T cell memory. *Annu. Rev. Immunol.* 20:551–579.
2. Wong, P., and E.G. Pamer. 2003. CD8 T cell responses to infectious pathogens. *Annu. Rev. Immunol.* 21:29–70.
3. Ahmed, R., and D. Gray. 1996. Immunological memory and protective immunity: understanding their relation. *Science.* 272:54–60.
4. Kaech, S.M., E.J. Wherry, and R. Ahmed. 2002. Effector and memory T-cell differentiation: implications for vaccine development. *Nat. Rev. Immunol.* 2:251–262.
5. Mercado, R., S. Vijh, S.E. Allen, K. Kerksiek, I.M. Pilip, and E.G. Pamer. 2000. Early programming of T cell populations responding to bacterial infection. *J. Immunol.* 165:6833–6839.
6. Kaech, S.M., and R. Ahmed. 2001. Memory CD8+ T cell differentiation: initial antigen encounter triggers a developmental program in naive cells. *Nat. Immunol.* 2:415–422.
7. Van Stipdonk, M.J., E.E. Lemmens, and S.P. Schoenberger. 2001. Naive CTLs require a single brief period of antigenic stimulation for clonal expansion and differentiation. *Nat. Immunol.* 2:423–429.
8. Badovinac, V.P., B.B. Porter, and J.T. Harty. 2002. Programmed contraction of CD8(+) T cells after infection. *Nat. Immunol.* 3:619–626.
9. Van Stipdonk, M.J., G. Hardenberg, M.S. Bijker, E.E. Lemmens, N.M. Droin, D.R. Green, and S.P. Schoenberger. 2003. Dynamic programming of CD8(+) T lymphocyte responses. *Nat. Immunol.* 4:361–365.
10. Blattman, J.N., J.M. Grayson, E.J. Wherry, S.M. Kaech, K.A. Smith, and R. Ahmed. 2003. Therapeutic use of IL-2 to enhance antiviral T-cell responses in vivo. *Nat. Med.* 9:540–547.
11. Badovinac, V.P., A.R. Tvinnereim, and J.T. Harty. 2000. Regulation of antigen-specific CD8+ T cell homeostasis by perforin and interferon-gamma. *Science.* 290:1354–1358.
12. van Lier, R.A., J. Borst, T.M. Vroom, H. Klein, P. Van Mourik, W.P. Zeijlemaker, and C.J. Melief. 1987. Tissue distribution and biochemical and functional properties of Tp55 (CD27), a novel T cell differentiation antigen. *J. Immunol.* 139:1589–1596.
13. Klein, U., K. Rajewsky, and R. Kuppers. 1998. Human im-

munoglobulin (Ig)M[+]IgD[+] peripheral blood B cells expressing the CD27 cell surface antigen carry somatically mutated variable region genes: CD27 as a general marker for somatically mutated (memory) B cells. *J. Exp. Med.* 188:1679–1689.

14. Sugita, K., M.J. Robertson, Y. Torimoto, J. Ritz, S.F. Schlossman, and C. Morimoto. 1992. Participation of the CD27 antigen in the regulation of IL-2-activated human natural killer cells. *J. Immunol.* 149:1199–1203.

15. Wiesmann, A., R.L. Phillips, M. Mojica, L.J. Pierce, A.E. Searles, G.J. Spangrude, and I. Lemischka. 2000. Expression of CD27 on murine hematopoietic stem and progenitor cells. *Immunity.* 12:193–199.

16. Hintzen, R.Q., S.M. Lens, M.P. Beckmann, R.G. Goodwin, D. Lynch, and R.A. van Lier. 1994. Characterization of the human CD27 ligand, a novel member of the TNF gene family. *J. Immunol.* 152:1762–1773.

17. Oshima, H., H. Nakano, C. Nohara, T. Kobata, A. Nakajima, N.A. Jenkins, D.J. Gilbert, N.G. Copeland, T. Muto, H. Yagita, and K. Okumura. 1998. Characterization of murine CD70 by molecular cloning and mAb. *Int. Immunol.* 10:517–526.

18. Tesselaar, K., Y. Xiao, R. Arens, G.M. van Schijndel, D.H. Schuurhuis, R.E. Mebius, J. Borst, and R.A. van Lier. 2003. Expression of the murine CD27 ligand CD70 in vitro and in vivo. *J. Immunol.* 170:33–40.

19. Hintzen, R.Q., S.M. Lens, K. Lammers, H. Kuiper, M.P. Beckmann, and R.A. van Lier. 1995. Engagement of CD27 with its ligand CD70 provides a second signal for T cell activation. *J. Immunol.* 154:2612–2623.

20. Gravestein, L.A., J.D. Nieland, A.M. Kruisbeek, and J. Borst. 1995. Novel mAbs reveal potent co-stimulatory activity of murine CD27. *Int. Immunol.* 7:551–557.

21. Goodwin, R.G., M.R. Alderson, C.A. Smith, R.J. Armitage, T. VandenBos, R. Jerzy, T.W. Tough, M.A. Schoenborn, T. Davis-Smith, K. Hennen, et al. 1993. Molecular and biological characterization of a ligand for CD27 defines a new family of cytokines with homology to tumor necrosis factor. *Cell.* 73:447–456.

22. Brown, G.R., K. Meek, Y. Nishioka, and D.L. Thiele. 1995. CD27-CD27 ligand/CD70 interactions enhance alloantigen-induced proliferation and cytolytic activity in CD8+ T lymphocytes. *J. Immunol.* 154:3686–3695.

23. Yamada, S., K. Shinozaki, and K. Agematsu. 2002. Involvement of CD27/CD70 interactions in antigen-specific cytotoxic T-lymphocyte (CTL) activity by perforin-mediated cytotoxicity. *Clin. Exp. Immunol.* 130:424–430.

24. Hendriks, J., L.A. Gravestein, K. Tesselaar, R.A. van Lier, T.N. Schumacher, and J. Borst. 2000. CD27 is required for generation and long-term maintenance of T cell immunity. *Nat. Immunol.* 1:433–440.

25. Arens, R., K. Tesselaar, P.A. Baars, G.M. van Schijndel, J. Hendriks, S.T. Pals, P. Krimpenfort, J. Borst, M.H. van Oers, and R.A. van Lier. 2001. Constitutive CD27/CD70 interaction induces expansion of effector-type T cells and results in IFNgamma-mediated B cell depletion. *Immunity.* 15:801–812.

26. Tesselaar, K., R. Arens, G.M. van Schijndel, P.A. Baars, M.A. van der Valk, J. Borst, M.H. van Oers, and R.A. van Lier. 2003. Lethal T cell immunodeficiency induced by chronic costimulation via CD27-CD70 interactions. *Nat. Immunol.* 4:49–54.

27. Mamalaki, C., T. Norton, Y. Tanaka, A.R. Townsend, P. Chandler, E. Simpson, and D. Kioussis. 1992. Thymic deple-

tion and peripheral activation of class I major histocompatibility complex-restricted T cells by soluble peptide in T-cell receptor transgenic mice. *Proc. Natl. Acad. Sci. USA.* 89:11342–11346.

28. Dalton, D.K., S. Pitts-Meek, S. Keshav, I.S. Figari, A. Bradley, and T.A. Stewart. 1993. Multiple defects of immune cell function in mice with disrupted interferon-gamma genes. *Science.* 259:1739–1742.

29. Altman, J.D., P.A. Moss, P.J. Goulder, D.H. Barouch, M.G. McHeyzer-Williams, J.I. Bell, A.J. McMichael, and M.M. Davis. 1996. Phenotypic analysis of antigen-specific T lymphocytes. *Science.* 274:94–96.

30. Haanen, J.B., M. Toebes, T.A. Cordaro, M.C. Wolkers, A.M. Kruisbeek, and T.N. Schumacher. 1999. Systemic T cell expansion during localized viral infection. *Eur. J. Immunol.* 29:1168–1174.

31. Schepers, K., M. Toebes, G. Sotthewes, F.A. Vyth-Dreese, T.A. Dellemijn, C.J. Melief, F. Ossendorp, and T.N. Schumacher. 2002. Differential kinetics of antigen-specific CD4+ and CD8+ T cell responses in the regression of retrovirus-induced sarcomas. *J. Immunol.* 169:3191–3199.

32. van Elden, L.J., M. Nijhuis, P. Schipper, R. Schuurman, and A.M. van Loon. 2001. Simultaneous detection of influenza viruses A and B using real-time quantitative PCR. *J. Clin. Microbiol.* 39:196–200.

33. Wolkers, M.C., G. Stoetter, F.A. Vyth-Dreese, and T.N. Schumacher. 2001. Redundancy of direct priming and cross-priming in tumor-specific CD8+ T cell responses. *J. Immunol.* 167:3577–3584.

34. Liu, L., A. Chahroudi, G. Silvestri, M.E. Wernett, W.J. Kaiser, J.T. Safrit, A. Komoriya, J.D. Altman, B.Z. Packard, and M.B. Feinberg. 2002. Visualization and quantification of T cell-mediated cytotoxicity using cell-permeable fluorogenic caspase substrates. *Nat. Med.* 8:185–189.

35. Harrington, L.E., M. Galvan, L.G. Baum, J.D. Altman, and R. Ahmed. 2000. Differentiating between memory and effector CD8 T cells by altered expression of cell surface O-glycans. *J. Exp. Med.* 191:1241–1246.

36. Croft, M. 2003. Co-stimulatory members of the TNFR family: keys to effective T-cell immunity? *Nat. Rev. Immunol.* 3:609–620.

37. Cerwenka, A., T.M. Morgan, A.G. Harmsen, and R.W. Dutton. 1999. Migration kinetics and final destination of type 1 and type 2 CD8 effector cells predict protection against pulmonary virus infection. *J. Exp. Med.* 189:423–434.

38. Yewdell, J.W., and J.R. Bennink. 1999. Immunodominance in major histocompatibility complex class I–restricted T lymphocyte responses. *Annu. Rev. Immunol.* 17:51–88.

39. Rahemtulla, A., W.P. Fung-Leung, M.W. Schilham, T.M. Kundig, S.R. Sambhara, A. Narendran, A. Arabian, A. Wakeham, C.J. Paige, R.M. Zinkernagel, et al. 1991. Normal development and function of CD8+ cells but markedly decreased helper cell activity in mice lacking CD4. *Nature.* 353:180–184.

40. Matloubian, M., R.J. Concepcion, and R. Ahmed. 1994. CD4+ T cells are required to sustain CD8+ cytotoxic T-cell responses during chronic viral infection. *J. Virol.* 68:8056–8063.

41. Janssen, E.M., E.E. Lemmens, T. Wolfe, U. Christen, M.G. von Herrath, and S.P. Schoenberger. 2003. CD4+ T cells are required for secondary expansion and memory in CD8+ T lymphocytes. *Nature.* 421:852–856.

42. Rogers, P.R., J. Song, I. Gramaglia, N. Killeen, and M. Croft. 2001. OX40 promotes Bcl-xL and Bcl-2 expression

and is essential for long-term survival of CD4 T cells. *Immunity.* 15:445–455.

43. Lee, H.W., S.J. Park, B.K. Choi, H.H. Kim, K.O. Nam, and B.S. Kwon. 2002. 4-1BB promotes the survival of CD8+ T lymphocytes by increasing expression of Bcl-xL and Bfl-1. *J. Immunol.* 169:4882–4888.

44. Gamadia L.E., E.M. van Leeuwen, E.B. Remmerswaal, S.L. Yong, S. Surachno, P.M. Wertheim-van Dillen, I.J. Ten Berge, and R.A. Van Lier. 2004. The size and phenotype of virus-specific T cell populations is determined by repetitive antigenic stimulation and environmental cytokines. *J. Immunol.* 172:6107–6114.

45. Nieland, J.D., Y.F. Graus, Y.E. Dortmans, B.L. Kremers, and A.M. Kruisbeek. 1998. CD40 and CD70 co-stimulate a potent in vivo antitumor T cell response. *J. Immunother.* 21:225–236.

46. Couderc, B., L. Zitvogel, V. Douin-Echinard, L. Djennane, H. Tahara, G. Favre, M.T. Lotze, and P.D. Robbins. 1998. Enhancement of antitumor immunity by expression of CD70 (CD27 ligand) or CD154 (CD40 ligand) costimulatory molecules in tumor cells. *Cancer Gene Ther.* 5:163–175.

47. Lorenz, M.G., J.A. Kantor, J. Schlom, and J.W. Hodge. 1999. Anti-tumor immunity elicited by a recombinant vaccinia virus expressing CD70 (CD27L). *Hum. Gene Ther.* 10:1095–1103.